

RESEARCH ARTICLE

Evaluation of Parameters Affecting the Inelastic Acceleration Ratio

Emad Elhout*

Associate Professor, Civil Engineering Department, Faculty of Engineering, Damanhour University, Egypt

* Corresponding author: Emad Elhout, emad_aliali@yahoo.com

ABSTRACT

The Inelastic Acceleration Ratio (IAR) is a helpful instrument for determining the maximum inelastic acceleration from the related elastic acceleration that seems to have been little examined in past research. The IARs using single-degree-of-freedom (SDOF) systems with various structural factors under thirty pairs of ground motion earthquakes recorded are investigated in this paper. The linear elastic-perfect plastic model is used to model SDOF systems. The factors to consider include elastic vibration period (T), displacement ductility ratios (μ , 2-8), the post-yield stiffness ratio (α , 0-15%), and the damping ratio (ξ , 3-20%). The results showed that the IAR values are decreased with an increase in the ductility ratios (μ) while the IAR values are increased with an increase in the damping ratios (ξ). While the post-yield stiffness ratio (α) has little effect on the IAR. Also, Analytical formulae are used to estimate IAR based on the T , μ , α , and ξ .

Keywords: The Inelastic Acceleration Ratio; damping ratio; the post-yield stiffness ratio the vibration period; ductility ratio

1. Introduction

Many studies are focused on evaluating the inelastic seismic response of building structures. This remains one of the most significant problems in structural engineering. So, the seismic performance evaluation of nonlinear structure analysis must be evaluated accurately to define the structure's reliable earthquake resistance. The seismic design of structures reduces collapse by allowing structural components to distribute seismic energy through inelastic deformations. Most studies use linear analysis using some parameters to predict the nonlinear responses of structures under seismic loads, such as using the inelastic spectra through parameters based on their elastic responses. The Inelastic Displacement Ratios (IDRs), Inelastic Velocity Ratios (IVRs), and Inelastic Acceleration Ratios (IARs) allow the computation of maximum inelastic displacements, velocities, and accelerations, respectively, without performing complicated inelastic analyses, direct from the equivalent elastic ones.

The maximum lateral displacement always predicted seismic design codes to evaluate the seismic demand of structure under earthquake based on elastic response spectrum which is based on the IDRs. The IDR is the SDOF system's maximum inelastic to maximum elastic displacement ratio. This factor has been used in prior investigations for achieving inelastic displacement without requiring nonlinear dynamic analysis. Hatzigeorgiou and Beskos^[1] presented a simple method to estimate the IDR of a structure under

ARTICLE INFO

Received: 21 June 2025 | Accepted: 22 July 2025 | Available online: 21 November 2025

CITATION

E. Elhout. Evaluation of Parameters Affecting the Inelastic Acceleration Ratio. *Earthquake*. 2025; 3(2): 8454. doi: 10.59429/ear.v3i2.8454

COPYRIGHT

Copyright © 2025 by author(s). *Earthquake* is published by Arts and Science Press Pte. Ltd. This is an Open Access article distributed under the terms of the Creative Commons Attribution License (<https://creativecommons.org/licenses/by/4.0/>), permitting distribution and reproduction in any medium, provided the original work is cited.

repeated or multiple earthquakes. Many parameters such as damping ratio, local site conditions, post-yield stiffness ratio, force reduction factors and the structural period of vibration are taken to find expressions for this ratio. It was found that the viscous damping ratio and local site conditions are not significantly affected in estimating the IDRs. The post-yield stiffness ratio, force reduction factors, and the structural period of vibration are influences on estimating the IDR.

Ruiz-García^[2] evaluated the IDR of SDOF systems subjected to near-fault ground motions. Also, an estimated equation to obtain the IDR for the seismic assessment of structures exposed to forward-directivity near-fault ground motions is proposed. The IDR of nonstructural components that were subjected to floor accelerations was examined by Obando and Lopez-Garcia^[3]. Chimneys, cooling systems, antennae, and barriers are some acceleration-sensitive nonstructural elements where the inelastic displacement demand is relevant. Chikh et al.^[4] estimated the IDR for SDOF bilinear systems by rigorous nonlinear analysis which depends on the period, the post to pre-yield stiffness ratio, the yield strength reduction factor, and the peak ground acceleration. De Francesco^[5] This paper focuses on constant-ductility IDR of SDOF systems with two different levels of energy dissipation capacity, in the presence of a 5% viscous damping ratio. The research includes 228 ground motions with magnitudes larger than six that were observed in California. The behavior of self-centering SDF systems with many parameters are studied and compared to those of SDF systems with bilinear plastic. The analysis indicated that Like in all the other hysteretic systems studied, the dispersion in the earthquake data is the number of inelastic displacement ratios of self-centering systems based on the aggregate effects of ductility, starting period, and post-yield stiffness ratio.

Yaghmaei-Sabegh et al.^[6] estimated the IDR of SDOF systems with damping ratios and post-yield stiffness ratios in underground motion records obtained at sites of soft soil. As a function of numerous parameters, a simplified equation has also been suggested using nonlinear regression analysis. It can be concluded that the effect of soil condition on the inelastic displacement ratio increases with increasing ductility level and the damping ratio. Dong et al.^[7] investigates the IDR of SDOF systems to the self-centering structure subjected to near- and far-fault ground motions. Different parameters such as ductility levels, peak ground velocity, site condition, and the natural period are used in this study. The results indicated that the post-yielding stiffness ratio, energy dissipation ratio, ductility factor, and vibration period have a significant effect on the inelastic displacement ratio. Moreover, a flag-shaped model has more effect on the inelastic displacement demands of the structure than the bilinear model and Modified Clough model. Additionally, a simplified formula is created to determine the IDR for self-centering structure design. Applying information regarding the IDR of SDOF systems with strength and stiffness degraded peak-oriented hysteretic theory and failure threat through nonlinear time history evaluations, BÖREKÇİ and AYDOĞAN (2024) provided Artificial Neural Network models. The results show that, for a given set of parameters, Artificial Neural Network approaches produce higher precision than earlier techniques and may be implemented for calculating the IDR.

As has already been indicated, a thorough analysis of the IDR's review has been done in the past. However, there hasn't been much research done on determining velocities for inelastic constructions that are exposed to severe earthquakes. It seems that evaluating velocities is important for many velocity-dependent nonlinear structures, especially inelastic constructions that have additional viscous dampers^[8] The ratio of an SDOF system's highest inelastic velocity to its maximum elastic velocity is known as the inelastic velocity ratio (IVR), according to Hatzigeorgiou and Papagiannopoulos^[9]. In addition to the equations for IVR as a function of the period of motion, damping ratio, force reduction factor, and soil type have been determined using substantial statistical research. A straightforward model utilizing the IVR was presented by Hatzigeorgiou and Pnevmatikos^[10] for the assessment of effective velocities and damping forces for SDOF

structures with additional viscous dampers during earthquakes. Under a dozen pulses record, Konstandakopoulou and Hatzigeorgiou^[11] examined the constant-ductility inelastic spectra ratios for SDOF systems. According to the analysis, the type of pulse and the number of cycles affect the IDR, IVR, and IAR. Designers can assess the inelastic behavior of constructions by directly computing the highest inelastic acceleration using the equivalent elastic one using the IAR, which is another helpful index.

An additional third ratio related to acceleration is the inelastic response ratio (IAR), defined as the ratio between the maximum inelastic accelerations and its elastic ones. This parameter is utilized to assess the seismic response of non-structural elements such as architectural, mechanical, electrical and plumbing element that are acceleration-sensitive component under earthquake ground motions^[12]. The inelastic acceleration ratio (IAR) was studied by Garakaninezhad and Amiri^[13] along with the influence of structural characteristics on this measure. These parameters include the elastic vibration period normalized by the pulse period, the strength modification factor, the viscous damping ratio, and the hysteretic principle. The chosen dataset contains ninety-one records of earthquakes. Moreover, mathematical formulas for estimating IAR due to the principal structural parameters and the normalized elastic vibration period are presented. These formulas can be utilized for the seismic assessment of non-structural and acceleration-sensitive buildings.

The IAR parameters were not examined a lot in much research for evaluating the inelastic buildings under seismic ground motion. So, the study aims to evaluate parameters affecting the inelastic acceleration ratio (IAR) of SDOF systems. The IARs using SDOF systems with various structural factors under thirty pairs of ground motion earthquakes recorded are investigated in this paper. The linear elastic-perfect plastic model is used to model SDOF systems. The factors to consider include elastic vibration period (T), displacement ductility ratios (μ , 2-8), the post-yield stiffness ratio (α , 0-15%), and the damping ratio (ξ , 3-20%). Also, analytical formulae are provided to estimate IAR as a function of T, μ , α , and ξ . This can be used to investigate the seismic performance of acceleration-sensitive structures and parts that are not structural.

2. Inelastic Acceleration Ratio (IAR)

The IAR (μ , T) is defined for constant-ductility inelastic spectra as the ratio between the maximum inelastic spectra accelerations and its elastic ones^[14]:

$$IAR(\mu, T) = \frac{SA(\mu, T)}{SA(\mu=1, T)} \quad (1)$$

This paper evaluates IARs using SDOF systems with a variety of structural factors. The factors to consider include elastic vibration period (T), displacement ductility ratios (μ), and the damping ratio (ξ). The software SeismoSignal version 4.3.0 determines the elastic and inelastic spectrum accelerations to all earthquake records. The examination of all the records of an earthquake has been carried through over 400 separate periods that go from 0.02 to 4.0 seconds. The linear elastic-perfectly plastic model is used to model SDOF systems, and the post-yield stiffness ratio is set to 0%, 5%, 10%, and 15%. The displacement ductility ratios (μ) used are 2, 4, 6, and 8. Consider damping ratios (ξ) of 3%, 5%, 10%, and 20%.

3. Database of strong motions Earthquake records

This study's analysis used thirty pairs of ground motion earthquakes recorded between 1971 and 1999 from the COSMOS Virtual Data Centre to a wide range of closest distances and seismic moment magnitudes. The earthquakes at the closest distance range from 2.31 to 106.8 km, the PGA (g) of the earthquake records

is between 0.02 and 1.5 and the moment magnitudes range from 5.2 to 7.5 as shown in figures (1 and 2). Table 1 presents the earthquake records and the associated data.

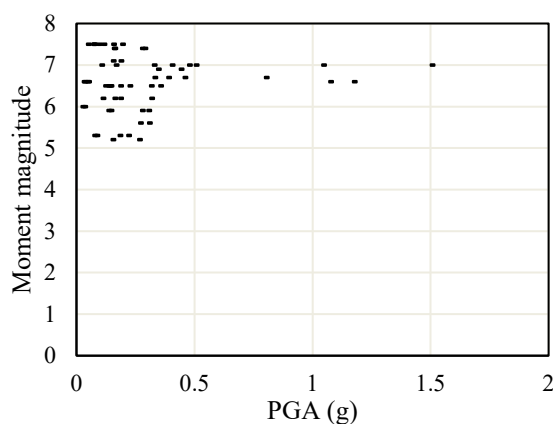
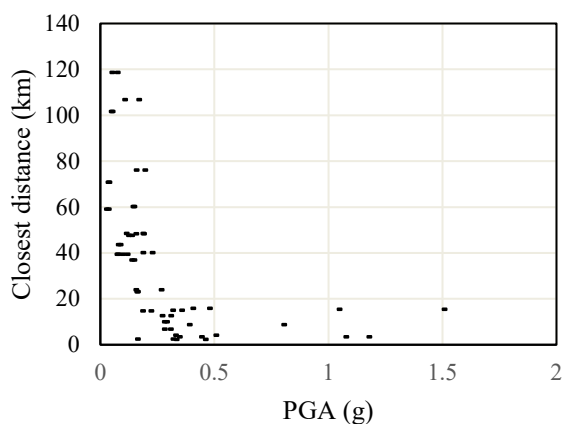


Figure 1. The relation between closest distance and PGA (g) of ground motion records.

Figure 2. The relation between the moment magnitude and PGA (g) of ground motion records.

Table 1. Data of earthquake records

NO	Earthquake name	Year	Station Name	Moment magnitude	Closest distance (km)	Site Geology	Com	A (g)	V (m/sec)
1	Joshua Tree/ Hector Mine	1999	Amboy	7.1	48.4	Alluvium	360	0.149	0.19
							90	0.182	0.27
2	Redding	1998	Redding, CA	5.2	24	-	90	0.26	0.094
							360	0.148	0.035
3	Northridge	1994	Saticoy ST	6.7	2.31	-	S00E	0.453	0.61
							S90E	0.325	0.31
4	Northridge	1994	Sylmar - 6-Story County Hospital	6.7	8.7	Alluvium	90	0.383	0.71
							0	0.797	11.2
5	Big Bear	1992	Desert Hot Springs	6.5	40.1	Deep Alluvium	360	0.18	0.16
							90	0.22	0.19
6	Cape Mendocino	1992	Cape Mendocino, CA – Petrolia	7.0	15.5	Cretaceous Rock	90	1.04	0.41
							0	1.5	1.26
7	Landers	1992	Joshua Tree	7.4	10	Alluvium	0	0.273	0.27
							90	0.283	0.42
8	Landers	1992	Pomona	7.5	118.7	Alluvium	90	0.044	0.085
							0	0.067	0.12
9	Landers	1992	Desert Hot Springs	7.4	23.1	Deep Alluvium	90	0.153	0.2
							150	0.156	0.12
10	Petrolia	1991	Eureka - Myrtle & West Avenue	6	59.1	Partly Cons Sediments	360	0.02	0.03
							90	0.028	0.02
11	Limon, Costa Rica	1991	San Jose – Guatuso	7.5	39.4	-	0	0.11	0.09
							270	0.07	0.06
12	Limon, Costa Rica	1991	San Isidro	7.5	76.1	Alluvium	270	0.15	0.09
							0	0.188	0.14
13	Limon, Costa Rica	1991	Puriscal	7.5	39.4	Alluvium	0	0.09	0.075
							270	0.066	0.076

NO	Earthquake name	Year	Station Name	Moment magnitude	Closest distance (km)	Site Geology	Com	A (g)	V (m/sec)
14	Sierra Madre	1991	Cogswell Dam	5.6	12.6	weathered granitic rock	155 65	0.302 0.264	0.14 0.096
15	Santa Cruz	1989	OLEMA	7.0	106.8	Alluvium	90 0	0.1 0.161	0.16 0.18
16	Santa Cruz Mtns	1989	Capitola - Fire Station	7.0	15.9	Alluvium	90 0	0.398 0.472	0.30 0.36
17	Santa Cruz Mtns	1989	Saratoga - Aloha Ave.	7.0	4.1	Alluvium	0 90	0.5 0.322	0.41 0.44
18	Whittier Aftershock	1987	Tarzana - Cedar Hill Nursery	5.3	43.6	Alluvium	90 0	0.08 0.071	0.04 0.029
19	Whittier Aftershock	1987	Fremont School	5.3	14.8	Alluvium	270 180	0.214 0.178	0.085 0.1
20	Palm Springs	1986	Desert Hot Springs	5.9	6.8	Deep Alluvium	0 90	0.3 0.273	0.33 0.18
21	Palm Springs	1986	Hemet - Stetson Ave Fire Station	5.9	36.9	Deep alluvium	360 270	0.14 0.13	0.05 0.048
22	Morgan	1984	Halls Valley	6.2	2.5	Alluvium	240 150	0.312 0.156	0.396 0.126
23	Coalinga	1983	Parkfield, CA - Cholame 5W	6.5	60.2	Sandstone	270 360	0.14 0.136	0.106 0.107
24	Mammoth Lakes	1980	Benton	6.2	48.5	Alluvium	360 270	0.18 0.106	0.11 0.072
25	Imperial Valley	1979	Coachella Canal Number 4	6.5	47.6	stiff soil	S45E N45E	0.13 0.116	0.15 0.12
26	Imperial Valley	1979	Huston Rd., El Centro Array #6, Ca	6.9	3.5	alluvium; more than 300m	S50W S40E	0.437 0.34	1.13 0.66
27	Friuli-Italy-01	1976	Tolmezzo	6.5	15.8		0 270	0.35 0.31	31 30
28	San Fernando	1971	Pacoima Dam, Cal.	6.6	3.5	Highly jointed Diorite Gneiss	S16E S74W	1.17 1.07	1.135 0.576
29	San Fernando	1971	Port Hueneme, Navy Laboratory, Cal.	6.6	70.8	Alluvium	S90W S00W	0.03 0.026	0.06 0.072
30	San Fernando	1971	San Bernardino, Cal	6.6	101.6	Alluvium	N00E N90E	0.04 0.045	0.035 0.027

Table 1. (Continued)

4. Inelastic Acceleration Ratio (IAR)

The IAR parameters obtained by the dynamic nonlinear analysis based on ground motion information are presented in the next subsection. The linear elastic-perfectly plastic model is used to model SDOF systems, and the post-yield stiffness ratio (α) is set to 0.0, 0.05, 0.1, and 0.15. The displacement ductility ratios (μ) used are 2, 4, 6, and 8. The damping ratios (ξ) are used at 3%, 5%, 10%, and 20%.

4.1. Variation of the mean IAR with the ductility ratio (μ)

The mean IAR -T spectra evaluated for this study's thirty pairs of ground motions as shown in Fig. 3. The spectra show SDOFs with $\xi = 5\%$, varying ductility ratios ($\mu=2, 4, 6,$ and 8) and post-yield stiffness ratios ($\alpha = 0.0, 0.05, 0.1,$ and 0.15). The results show that μ considerably impacts a considerable impact on the mean IAR. Increasing μ causes a decrease in IAR over a given period. These results are consistent with Konstandakopoulou and Hatzigeorgiou^[15].

Figure 3 further shows that the mean IAR is significantly reliant on T in the short-period time region of 0 to 0.1 seconds for all α levels. The spectrum seems to be a sequence of straight lines in this region. However, for periods greater than 0.1 seconds, the mean IAR is roughly period independent. IAR has shown a general tendency to increase as the period of the systems increases for periods greater than 0.1 sec and these results are consistent with Konstandakopoulou and Hatzigeorgiou^[16]. Also, the mean IAR is significantly increasing by increasing α , especially for high ductility ratio.

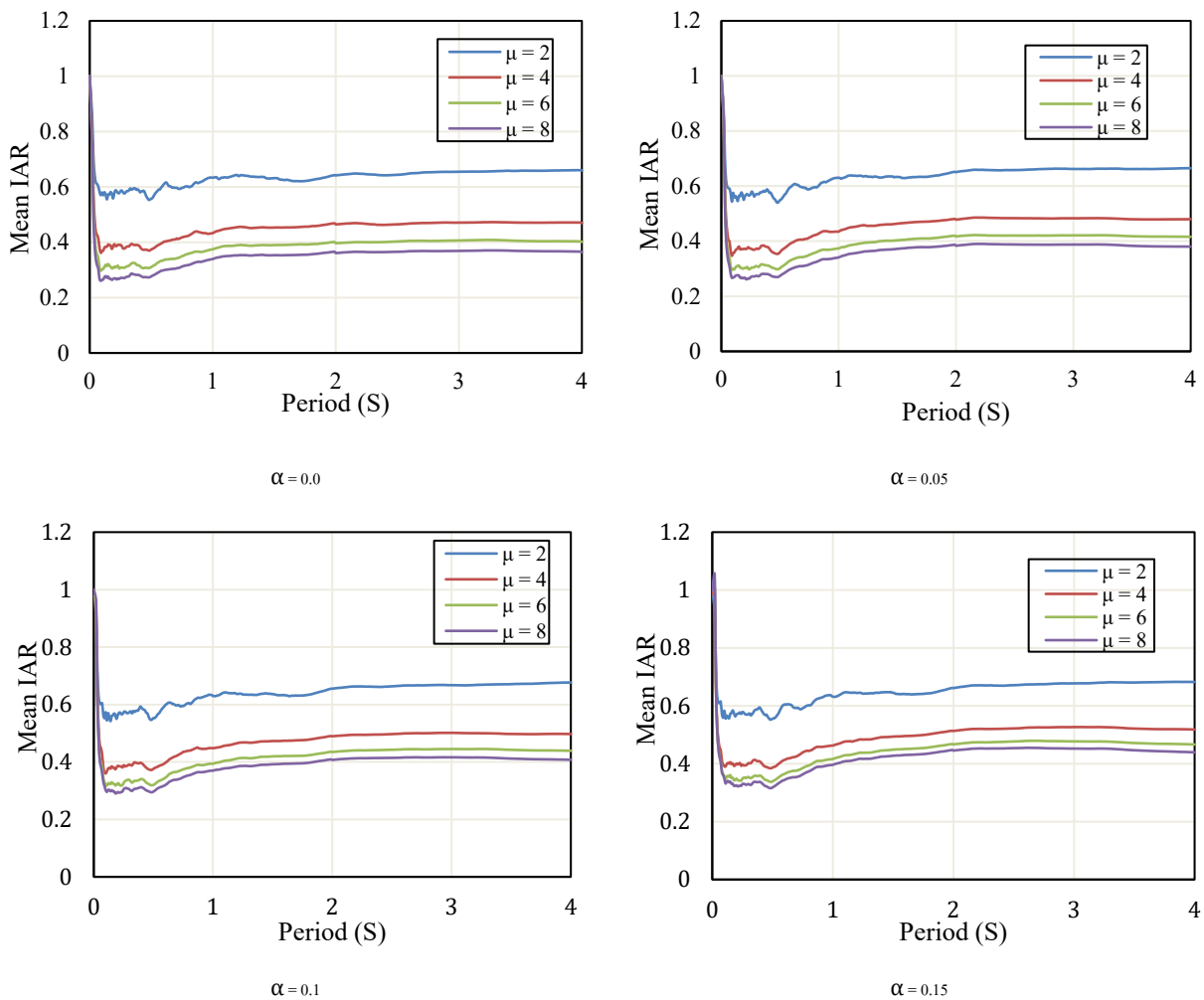


Figure 3. The mean IAR varies with μ for SDOFs with varying α and 5% damping.

Figure 4 shows the mean IAR -T spectra for SDOFs with post-yield stiffness ratio α equal to 0.1 and different ductility ratios ($\mu = 2, 4, 6,$ and 8) and damping ratios ($\xi = 3\%, 5\%, 10\%,$ and 20%). Fig. 4 shows results that are consistent with those in Figure 3. The mean IAR is dependent on T in the short-period range and increasing the μ causes a decrease in IAR over a given period. The spectrum seems to be a sequence of

straight lines in this region. The results show that the ξ considerably a considerable impact on the mean *IAR*. Increasing the ξ causes an increase in *IAR* over a given period for all values of μ . These results are consistent with the results of Konstandakopoulou and Hatzigeorgiou^[15].

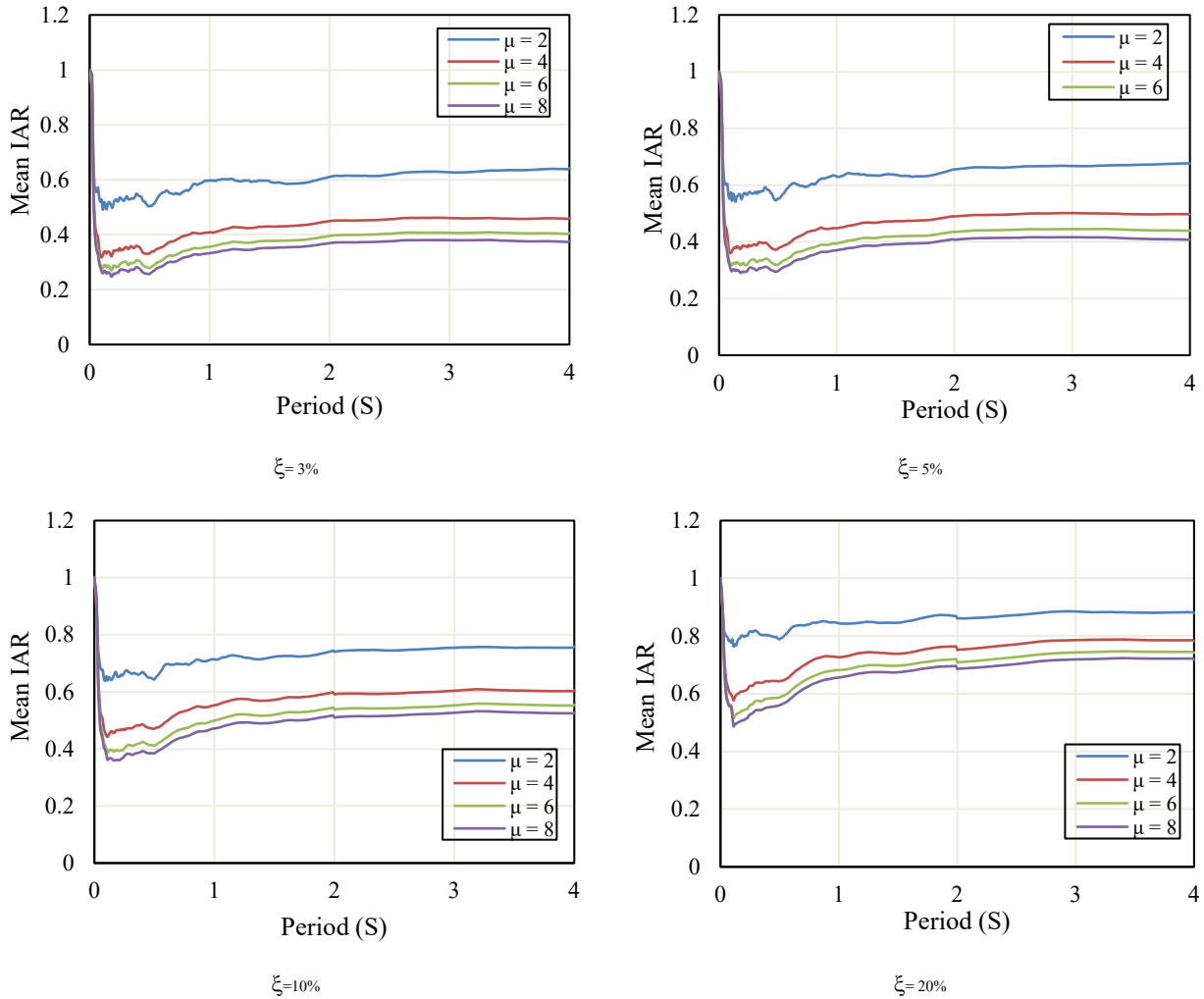


Figure 4. The mean IAR varies with μ for SDOFs with varying ξ and with α equals to 0.1.

4.2. The Variation of the mean IAR with the post-yield stiffness ratio (α)

The mean IAR -T spectra evaluated for this study's thirty pairs of ground motions as shown in Figure 5. The spectra show SDOFs with $\xi = 5\%$, varying ductility ratios ($\mu=2, 4, 6, \text{ and } 8$), and post-yield stiffness ratios ($\alpha = 0.0, 0.05, 0.1, \text{ and } 0.15$). The results show that the mean *IAR* is independent of α , especially for SDOFs with low ductility ratios. The α has a significant impact on mean *IAR* for SDOFs with large ductility ratios and periods longer than 0.1 sec.

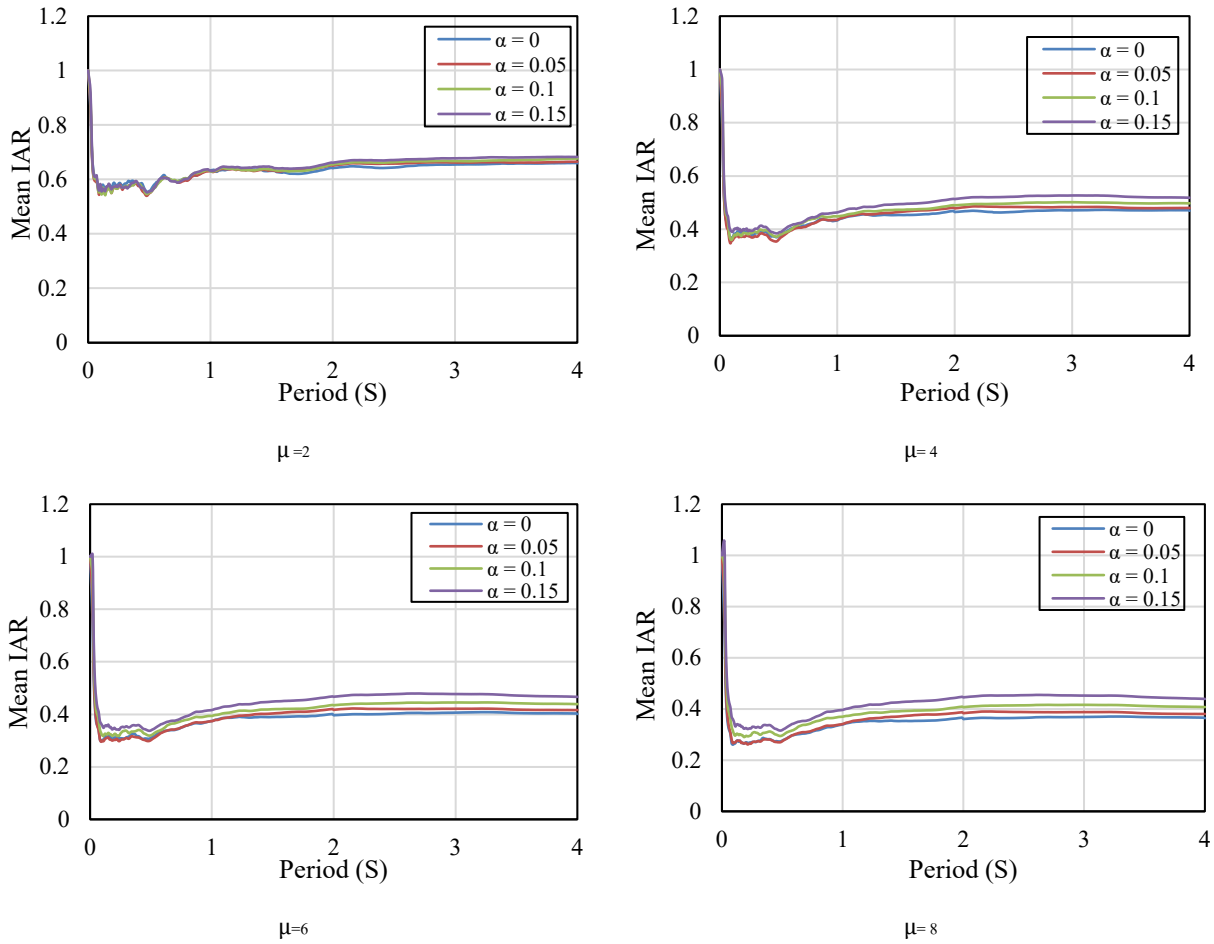


Figure 5. The mean IAR varies with α for SDOFs with varying μ with ξ equals 5%.

The mean IAR -T spectra evaluated for this study's thirty pairs of ground motions as shown in Figure 6. The spectra show SDOFs with μ equal to 6, varying damping ratios ($\xi = 3\%$, 5% , 10% , and 20%), and post-yield stiffness ratios ($\alpha = 0.0, 0.05, 0.1, \text{ and } 0.15$). The results presented in Fig.10 indicate that the mean IAR is roughly independent of the α in cases of SDOFs with $\xi = 10\%$, and 20% . The effect of the stiffness ratio α on the mean IAR is only pronounced for SDOFs with $\xi = 3\%$ and 5% . The study found that for SDOFs with high damping ratios, the mean IAR is mostly independent of α . The α has a significant impact on mean IAR for SDOFs with low damping ratios in periods longer than 0.1 sec. Figs. 5 and 6 show that the effect of α on mean IAR is only significant for SDOFs with low ductility ratios and high damping ratios. In SDOFs with high ductility ratios and low damping ratios, increasing the α leads to a rise in the mean IAR.

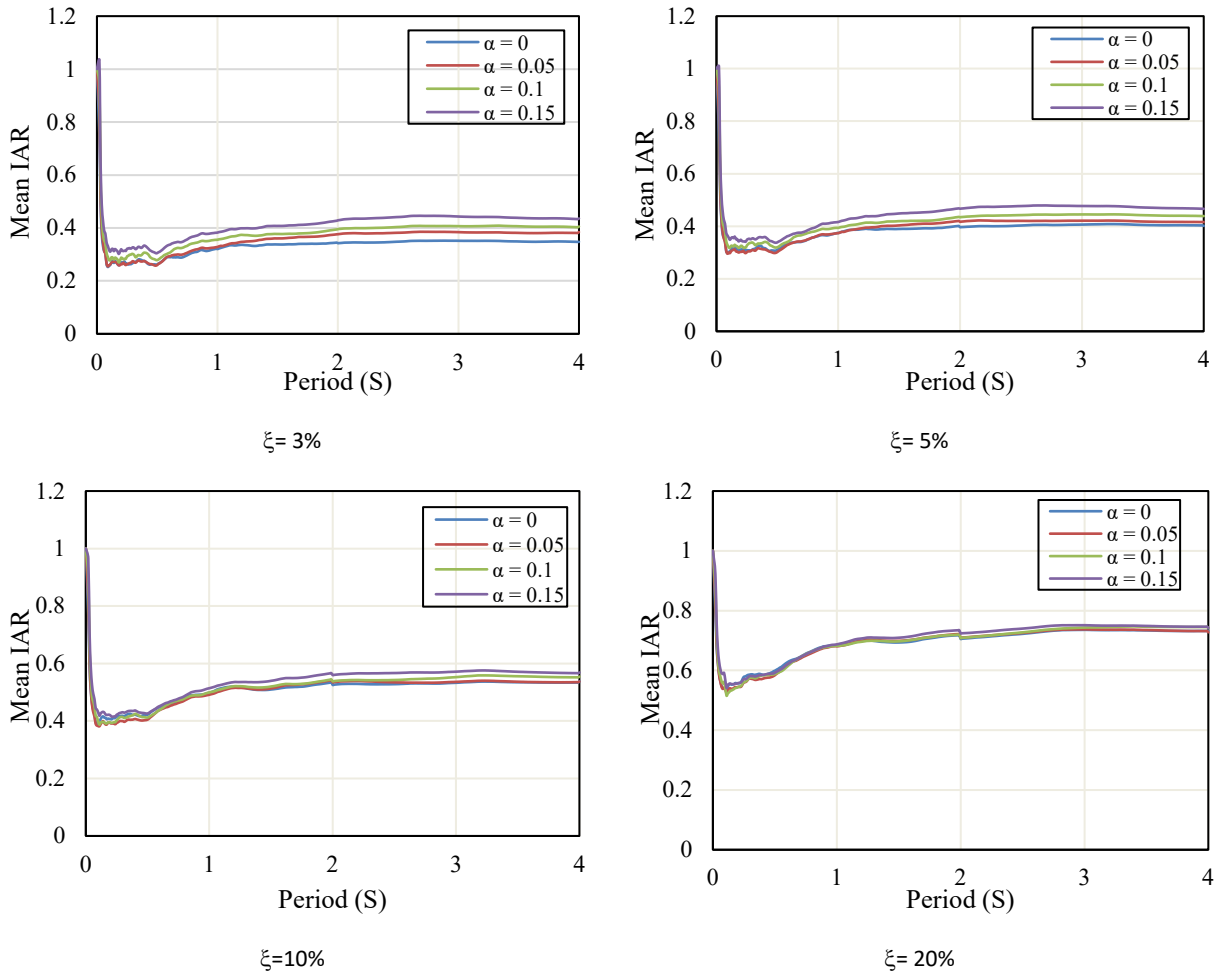


Figure 6. The mean IAR varies with α for SDOFs with varying ξ and with μ equal to 6.

4.3. The Variation of the mean IAR with the viscous damping ratio (ξ)

The mean IAR -T spectra evaluated for this study's thirty pairs of ground motions as shown in Figure 7. The spectra show SDOFs with α equal to 0.1, varying damping ratios ($\xi = 3\%, 5\%, 10\%,$ and 20%), and ductility ratios ($\mu = 2, 4, 6,$ and 8). Fig. 7 shows that ξ affect the mean IAR value. The ξ have a greater impact on the mean IAR in SDOFs with high ductility ratios. Increasing ξ leads to an increase in IAR over time, regardless of ductility ratio (μ).

The results show that the mean IAR is relatively independent of ξ , especially for SDOFs with periods shorter than 0.1 sec. The spectrum seems to be a sequence of straight lines in this region. Damping ratios (ξ) have a significant impact on mean IAR for SDOFs with ductility ratios lasting more than 0.1 second.

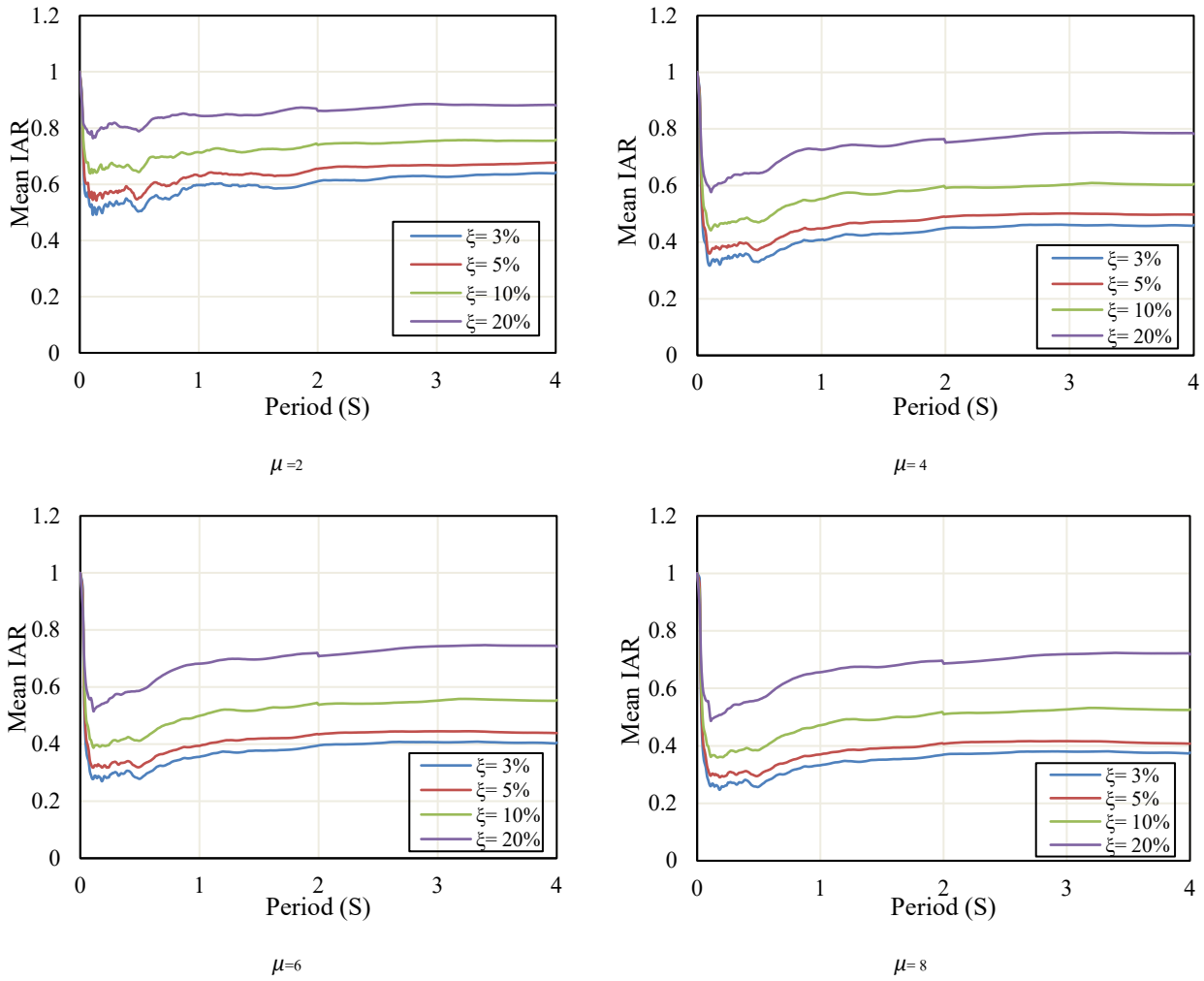
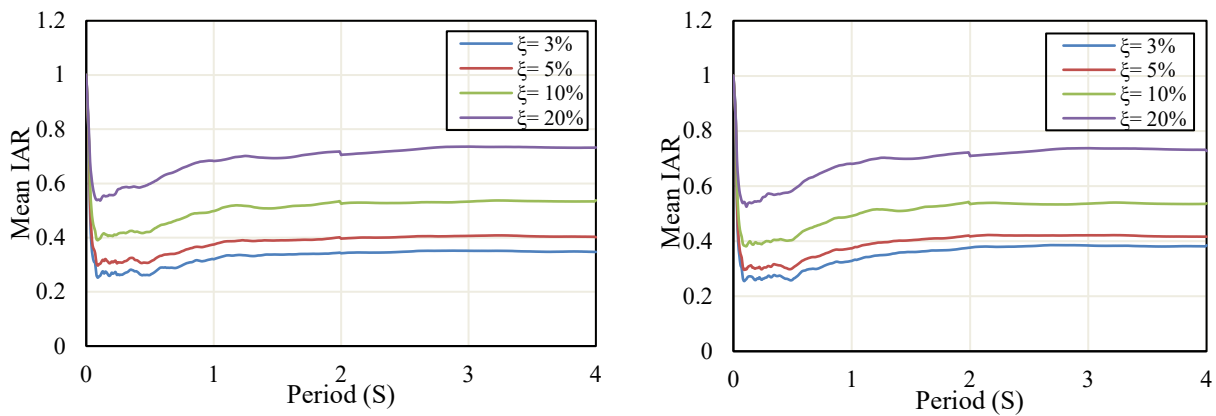


Figure 7. The mean IAR varies with ξ for SDOFs with varying μ and with α equal to 0.1.

The mean IAR -T spectra evaluated for this study's thirty pairs of ground motions as shown in Figure 8. The spectra show SDOFs with μ equal to 6, varying damping ratios ($\xi=3\%$, 5% , 10% , and 20%), and the post-yield stiffness ratio ($\alpha=0.0, 0.05, 0.1$, and 0.15). Fig. 8's results are consistent with those shown in Fig. 7. The ξ is an effect on the mean IAR of the SDOF system that the mean IAR is increased by increasing the ξ for all stiffness ratio α levels.



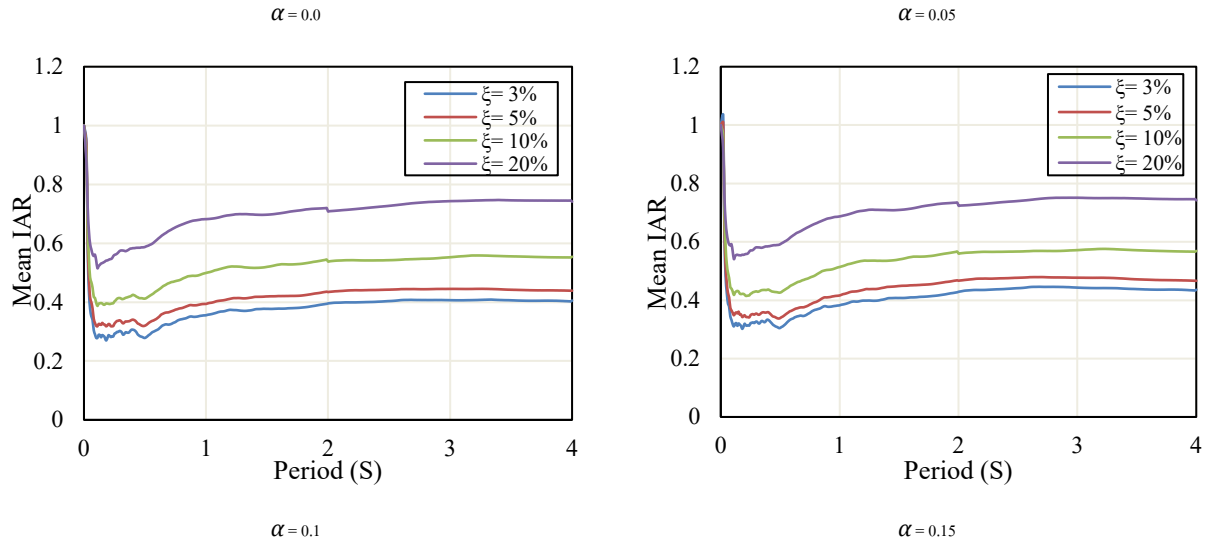


Figure 8. The mean IAR varies with ξ for SDOFs with varying α and with μ equals 6.

5. Prediction equations of IAR

For each SDOF system evaluated in this investigation, an individual mean *IAR* value is determined by the average mean *IAR* values over periods of less than 0.10 sec and longer than 0.1 sec. Tables 2 and 3 represent the mean *IAR* for SDOFs with varying α , ξ , and μ values for periods less than 0.10 sec and higher than 0.1 sec, respectively.

Table 2. Mean IAR of SDOF systems having different α , ξ , and μ along the period less than 0.10 sec.

α	$\xi = 3\%$				$\xi = 5\%$				$\xi = 10\%$				$\xi = 20\%$			
	$\mu = 2$	$\mu = 4$	$\mu = 6$	$\mu = 8$	$\mu = 2$	$\mu = 4$	$\mu = 6$	$\mu = 8$	$\mu = 2$	$\mu = 4$	$\mu = 6$	$\mu = 8$	$\mu = 2$	$\mu = 4$	$\mu = 6$	$\mu = 8$
0.0	0.601	0.437	0.379	0.347	0.641	0.477	0.417	0.382	0.715	0.557	0.495	0.459	0.817	0.674	0.611	0.581
0.05	0.595	0.438	0.391	0.367	0.631	0.472	0.423	0.398	0.706	0.546	0.491	0.464	0.813	0.664	0.610	0.585
0.10	0.598	0.458	0.423	0.413	0.635	0.493	0.457	0.444	0.704	0.556	0.514	0.498	0.806	0.661	0.618	0.604
0.15	0.608	0.485	0.462	0.460	0.643	0.517	0.492	0.488	0.709	0.578	0.548	0.541	0.807	0.675	0.646	0.639

Table 3. Mean IAR of SDOF systems having different α , ξ , and μ along the period greater than 0.10 sec.

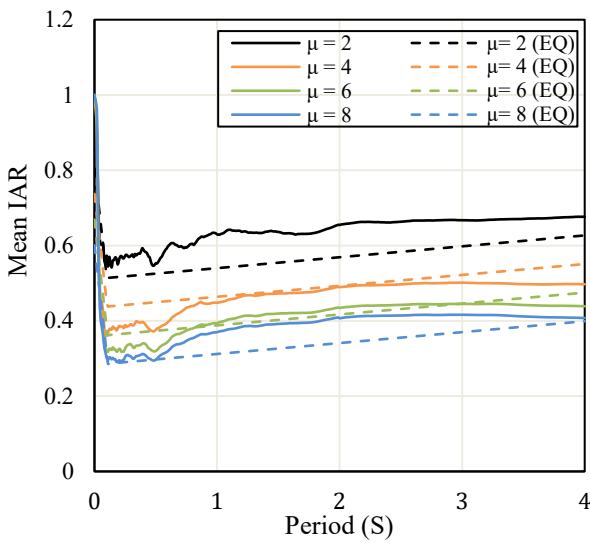
α	$\xi = 3\%$				$\xi = 5\%$				$\xi = 10\%$				$\xi = 20\%$			
	$\mu = 2$	$\mu = 4$	$\mu = 6$	$\mu = 8$	$\mu = 2$	$\mu = 4$	$\mu = 6$	$\mu = 8$	$\mu = 2$	$\mu = 4$	$\mu = 6$	$\mu = 8$	$\mu = 2$	$\mu = 4$	$\mu = 6$	$\mu = 8$
0.0	0.589	0.398	0.332	0.295	0.635	0.451	0.385	0.348	0.728	0.569	0.509	0.476	0.859	0.745	0.697	0.669
0.05	0.599	0.417	0.355	0.323	0.638	0.458	0.396	0.363	0.728	0.568	0.509	0.478	0.860	0.745	0.697	0.670
0.10	0.601	0.430	0.377	0.351	0.642	0.471	0.416	0.388	0.729	0.573	0.519	0.492	0.859	0.747	0.701	0.676
0.15	0.613	0.455	0.409	0.388	0.650	0.492	0.444	0.421	0.733	0.584	0.537	0.514	0.861	0.751	0.709	0.687

The following part provides the IAR's prediction formulas. Mathematical formulae for predicting the IAR of SDOF systems under 30 pairs of ground motion earthquakes using the linear elastic-perfect plastic model have been provided as an expression of T , μ , α , and ξ . The results presented two equations, the first to determine the *IAR* for the period structural systems less than 0.10 sec., and the second for the period structural systems greater than 0.10 sec. Table 4 summarizes all the suggested formulas.

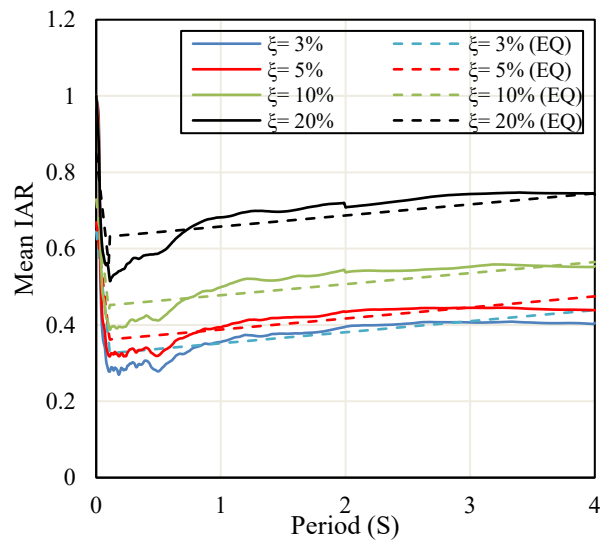
Table 4. Proposed IAR equations

NO.	Cases	Equations	The coefficient of determination (R ²)
1	$T \leq 0.10$ sec	$IAR = 0.813 - 2.88 (T) - 0.034(\mu) + 0.012 (\xi) + 0.002 (\alpha)$	0.67
2	$T > 0.10$ sec	$IAR = 0.497 + 0.029 (T) - 0.038(\mu) + 0.018 (\xi) + 0.002 (\alpha)$	0.92

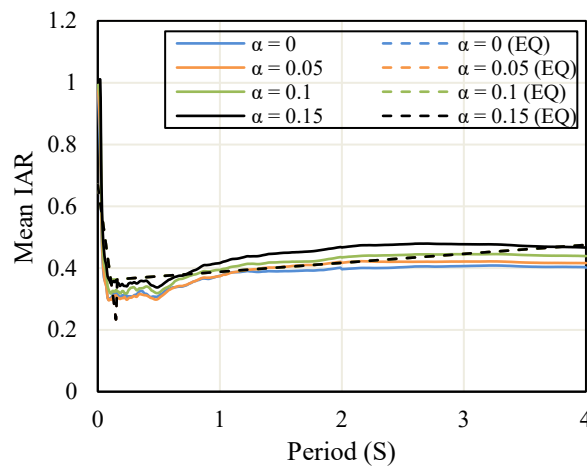
Where, T = the elastic vibration period, μ = displacement ductility ratios, α = the post-yield stiffness ratio, and ξ = the damping ratio. Figure 9 shows Konstandakopoulou and Hatzigeorgiou's (2020) estimated *IAR* results to the suggested *IAR* equations produced in the current research for various α , ξ and μ values. Konstandakopoulou and Hatzigeorgiou's ^[16] *IAR* is consistent with the suggested formulas for various α , ξ and μ values.



The mean IAR varies with μ for SDOFs with $\xi = 5\%$ and $\alpha = 0.1$



The mean IAR varies with ξ for SDOFs with $\mu = 6$ and $\alpha = 0.1$.



The mean IAR varies with α for SDOFs with $\xi = 5\%$ and $\mu = 6$

Figure 9. Proposed IAR equations.

6. Conclusion

This study aims to evaluate the IAR of SDOF systems with a variety of structural factors under thirty pairs of ground motion earthquakes recorded. The linear elastic-perfect plastic model is used to model SDOF systems. The factors to consider include elastic vibration period (T), displacement ductility ratios (μ , 2-8), the post-yield stiffness ratio (α , 0-15%), and the damping ratio (ξ , 3-20%). According to the outcomes derived from this research's evaluations, the results that follow can be reached:

- The post-yield stiffness ratio (α) has little effect on the *IAR*.
- The *IAR* values are decreased with an increase the ductility ratios (μ) over a given period for all values of the damping ratios (ξ) and all post-yield stiffness ratio (α) levels.
- The *IAR* values are increased with an increase the damping ratios (ξ) over a given period for all values of the ductility ratios (μ) and all post-yield stiffness ratio (α) levels.
- The mean *IAR* is significantly reliant on T in the short-period time region of 0 to 0.1 seconds for all stiffness ratio (α) levels.
- The mean *IAR* has shown a general tendency to increase as the period of the systems increases for periods greater than 0.1 sec.
- The *IAR* determined by Konstandakopoulou and Hatzigeorgiou (2020) agrees with the presented equations for various α , ξ , and μ levels.

The conclusions of this study rely on pairs of thirty ground motion earthquakes to calculate IAR, thus it is worth noting. More research on the effect of additional ground motion earthquake characteristics such as the PGA/PGV ratio, soil type, and earthquake magnitude levels on IAR.

Conflict of interest

The authors declare no conflict of interest

References

1. BÖREKÇİ M, AYDOĞAN B (2024) Prediction of inelastic displacement ratios for evaluation of degrading SDOF systems: A comparison of the scaled conjugate gradient and Bayesian regularized artificial neural network modeling. *Sigma Journal of Engineering and Natural Sciences* 42(1): 211-224. <https://doi.org/10.14744/sigma.2024.00018>
2. COSMOS (2017) The Consortium of Organizations for Strong-Motion Observation Systems. [http:// www.cosmos-eq.org/](http://www.cosmos-eq.org/)
3. Chikh B, Ahmed M, Nacer L, Moussa L, Youcef M, Mohamed H, Abderrahmane K, Djilali B (2017) Seismic structural demands and inelastic deformation ratios: a theoretical approach. *Earthquakes and Structures* 12 (4): 397-407. <https://doi.org/10.12989/eas.2017.12.4.397>
4. De Francesco G (2019) Constant-ductility inelastic displacement ratios for displacement-based seismic design of self-centering structures. *Earthquake Engineering Structure Dynamic* 48:188–209.
5. Dong H, Han Q, Du X, Liu J (2020) Constant ductility inelastic displacement ratios for the design of self-centering structures with flag-shaped models subjected to pulse-type ground motions. *Soil Dynamics and Earthquake Engineering* 133: 106143.
6. Federal Emergency Management Agency- FEMA450 (2003) NEHRP Recommended Provisions for Seismic Regulations for New Buildings and Other Structures, Part 1: Provisions and Part 2: Commentary, Washington D.C.
7. Garakaninezhad A, Amiri S (2022) Inelastic acceleration ratio of structures under pulse-like earthquake ground motions. In *Structures* 44: 1799-1810. <https://doi.org/10.1016/j.istruc.2022.08.102>

8. Hatzigeorgiou GD, Beskos DE (2009) Inelastic displacement ratios for SDOF structures subjected to repeated earthquakes. *Engineering Structures* 31(11):2744–55.
9. Hatzigeorgiou GD, Papagiannopoulos GA. Inelastic velocity ratio. *Earthquake Eng Struct Dyn* 2012; 41:2025–41.
10. Hatzigeorgiou GD, Pnevmatikos NG (2014) Maximum damping forces for structures with viscous dampers under near-source earthquakes. *Eng Struct* 68:1–13. <http://dx.doi.org/10.1016/j.engstruct.2014.02.036>
11. Kam WY, Pampanin S, Palermo A, Carr AJ (2010) Self-centering structural systems with combination of hysteretic and viscous energy dissipations. *Earthquake Engineering and Structural Dynamics* 39(10):1083–1108.
12. Konstandakopoulou F, Hatzigeorgiou G (2020) Constant-ductility inelastic displacement, velocity and acceleration ratios for systems subjected to simple pulses. *Soil Dyn Earthquake Eng* 131:106027. <https://doi.org/10.1016/j.soildyn.2019.106027>
13. Obando JC, Lopez-Garcia D (2016) Inelastic displacement ratios for nonstructural components subjected to floor accelerations. *Journal of Earthquake Engineering*, 1–26. <https://doi.org/10.1080/13632469.2016.1244131>
14. Pardalopoulos SI, Pantazopoulou SJ (2015) Seismic response of nonstructural components attached on multistorey buildings. *Earthq Eng Struct Dyn* 44(1): 139–58. <https://doi.org/10.1002/eqe.2466>
15. Ruiz-García J (2011) Inelastic displacement ratios for seismic assessment of structures subjected to forward-directivity near-fault ground motions. *Journal of Earthquake Engineering* 5: 449–68.
16. SeismoSignal, version 4.3.0, Pavia, Italy: Seismosoft Ltd. Retrieved from <http://www.seismosoft.com/en/HomePage.aspx>
17. Yaghmaei-Sabegh S, Daneshgari S, Neekmanesh S (2020) Inelastic displacement ratio for high damping SDOF systems built on soft soil sites. *Soil Dynamics, and Earthquake Engineering* 135: 106203. <https://doi.org/10.1016/j.soildyn.2020.106203>